Signal Processing 90 (2010) 1510–1517

Contents lists available at ScienceDirect

Signal Processing

journal homepage: www.elsevier.com/locate/sigpro

A neutrosophic approach to image segmentation based on watershed method

Ming Zhang [a], Ling Zhang [b], H.D. Cheng [a,*]

[a] Department of Computer Science, Utah State University, Logan, UT 84322, USA
[b] School of Mathematics and System Sciences, Shandong University, Jinan, Shandong 250100, PR China

ARTICLE INFO

Article history:
Received 7 June 2009
Received in revised form
23 October 2009
Accepted 24 October 2009
Available online 31 October 2009

Keywords:
Neutrosophy
Watershed
Image segmentation
Homogeneity
Indeterminacy

ABSTRACT

Neutrosophy studies the origin, nature, scope of neutralities, and their interactions with different ideational spectra. It is a new philosophy to extend the fuzzy logic and is the basis of neutrosophic logic, neutrosophic probability, neutrosophic set, and neutrosophic statistics.

Image segmentation is a key step for image processing, pattern recognition, computer vision. Many existing methods for image description, classification, and recognition highly depend on the segmentation results.

In this paper, neutrosophy is applied to image processing by defining a neutrosophic domain, which is described by three subsets T, I, and F. Then we employ watershed algorithm to perform segmentation of the image in the neutrosophic domain. The experiments show that the proposed method can get better results comparing with that obtained by the existing methods.

1. Introduction

Neutrosophy is a branch of philosophy [1], which includes four fields: philosophy, logics, set theory, and probability/statistics. It can solve some problems that cannot be solved by the fuzzy logic [2,3]. For example, two persons review a paper; both grade the paper as 80% acceptable. But the two reviewers may have different level of the background knowledge. One is an expert, and the other may be a fresh researcher in this field. The same acceptable percentage of these two reviewers should not have the same impact on the final consideration of the paper. There exist a lot of problems with indeterminacy such as weather forecast, presidential election, sport games, etc. Fuzzy logic cannot handle the indeterminate conditions well [4]. Neutrosophy introduces ⟨Neut-A⟩ to represent the indeterminacy.

Image segmentation is one of the most critical tasks of image analysis [5]. The segmentation results will affect the subsequent process of the image analysis and understanding, such as object representation and description, feature measurement, object classification, scene interpretation, etc. Image segmentation is a process of partitioning an image into multiple regions. It is typically used to locate objects and boundaries (lines, curves, etc.). The goal of segmentation is to make the representation of an image more meaningful and easier to analyze [6]. The popular approaches for image segmentation are histogram-based methods, edge-based methods, region-based methods, model based methods, and watershed methods [7–10]. Table 1 is the comparison of these methods. In this paper, we will propose a novel segmentation algorithm based on watershed method.

The original idea of watershed came from geography [11]. It is a powerful and popular image segmentation method [11–15] and can potentially provide more accurate segmentation with low computation cost [16]. The watershed algorithm splits an image into areas based on the topology of the image. The value of the gradients is interpreted as the

* Corresponding author.
E-mail address: hd.cheng@aggiemail.usu.edu (H.D. Cheng).

0165-1684/$ - see front matter © 2009 Elsevier B.V. All rights reserved.
doi:10.1016/j.sigpro.2009.10.021

Table 1
Comparison of segmentation methods.

Method	Description	Advantage	Disadvantage
Histogram-based	Find peaks and valleys in the histogram of the image and locate the clusters in the image	Fast and simple	Difficult to identify significant peaks and valleys
Edge-based	Find region boundaries	Fast and well-developed	Edges are often disconnected
Region-based	Use seeded region growing method	Resulting regions are connected	The choice of seeds is important and critical
Model-based	Find the interested regions by using geometry	Find a certain shape regions	The regions need to fit certain model
Watershed	Considers image as topographic surface	No seed is needed. Resulting regions are connected. Can find optimal boundaries	Sensitive to noise and inhomogeneity

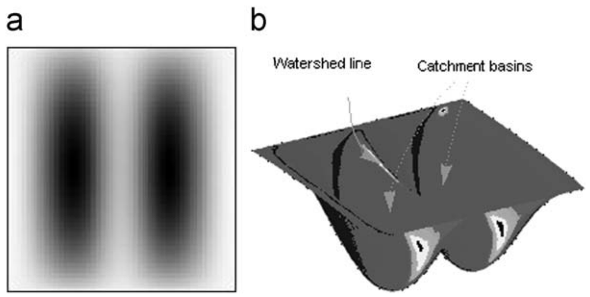

Fig. 1. Watershed concept: (a) two dark blobs and (b) 3D view of the watershed image of (a).

elevation information. After successively flooding the grey value, the watersheds with adjacent catchment basins are constructed. Fig. 1(a) is an image with two dark blobs synthetically generated by Matlab, and Fig. 1(b) is the 3D watershed image obtained by applying the watershed method on Fig. 1(a). Because the watershed methods work better on uniform images, our approach mainly deals with uniform image with blurry edges. However, our watershed method can also work better on non-uniformed images than other watershed methods.

In this paper, an image is mapped to neutrosophic domain. Then the neutrosophic logic is applied to convert the image into a binary image. Finally, the watershed algorithm is used to segment the converted image. We compare our proposed approach with the pixel-based method (embedded confidence), edge-based method (Sobel), region-based method (mean-shift), and two watershed methods (watershed in Matlab and toboggan-based [17]) in the experiments.

2. Neutrosophic set

Neutrosophic set is a generalization of the intuitionistic set [18], fuzzy set [4], paraconsistent set [19], dialetheist set [20], paradoxist set [1], and tautological set [1].

$\langle A \rangle$ is an event or entity, $\langle$Non-A$\rangle$ is not $\langle A \rangle$, and $\langle$Anti-A$\rangle$ is the opposite of $\langle A \rangle$. Also $\langle$Neut-A$\rangle$ is defined as neither $\langle A \rangle$ nor $\langle$Anti-A$\rangle$. For example, if $\langle A \rangle$=white, then $\langle$Anti-A$\rangle$=black. $\langle$Non-A$\rangle$=blue, yellow, red, black, etc. (any color except white). $\langle$Neut-A$\rangle$=blue, yellow, red, etc. (any color except white and black).

Define *T*, *I*, and *F* as neutrosophic components to represent $\langle A \rangle$, $\langle$Neut-A$\rangle$, and $\langle$Anti-A$\rangle$. Let *T*, *I* and *F* be standard or non-standard real subsets of $]^-0, 1^+[$ with $sup\,T = t\_sup$, $inf\,T = t\_inf$, $sup\,I = i\_sup$, $inf\,I = i\_inf$, $sup\,F = f\_sup$, $inf\,F = f\_inf$, and $n\_sup = t\_sup + i\_sup + f\_sup$, $n\_inf = t\_inf + i\_inf + f\_inf$ [21]. *T*, *I*, and *F* are not necessarily intervals, but may be any real sub-unitary subsets. *T*, *I*, and *F* are set-valued vector functions or operations depending on known or unknown parameters and may be continuous or discrete. They may overlap or be converted from one to the other [1]. An element $A(T, I, F)$ belongs to the set in the following way: it is *t* true ($t \in T$), *i* indeterminate ($i \in I$), and *f* false ($f \in F$), where *t*, *i*, and *f* are real numbers in the sets *T*, *I*, and *F*.

In this paper, an image is transferred to the neutrosophic domain. A pixel in the neutrosophic domain can be represented as $P\{T, I, F\}$, which means the pixel is *t*% true, *i*% indeterminate and *f*% false, where *t* varies in *T*, *i* varies in *I*, and *f* varies in *F*, respectively. In classical set: *i*=0, *t* and *f* are either 0 or 100. In fuzzy set: *i*=0, $0 \le t, f \le 100$. In neutrosophic set: $0 \le t, i, f \le 100$.

3. Proposed method

Watershed image segmentation is good for handling uniformed background and objects with blurry edges. In this paper, objects are *T* and background is *F*. The blurry edges are gradually changed from objects to background, and there are no clear boundaries between the objects and edges or between the background and edges. The blurry boundaries are defined in *I*.

3.1. Map image and decide $\{T, F\}$

Given an image *A*, $P(x, y)$ is a pixel in the image, and (x, y) is the position of this pixel. A 20×20 mean filter is applied to *A* for removing noise and making the image uniform. Then the image is converted by using the S-function:

$$T(x,y) = S(g_{xy}, a, b, c) = \begin{cases} 0 & 0 \le g_{xy} \le a \\ \dfrac{(g_{xy}-a)^2}{(b-a)(c-a)} & a \le g_{xy} \le b \\ 1 - \dfrac{(g_{xy}-c)^2}{(c-b)(c-a)} & b \le g_{xy} \le c \\ 1 & g_{xy} \ge c \end{cases} \quad (1)$$

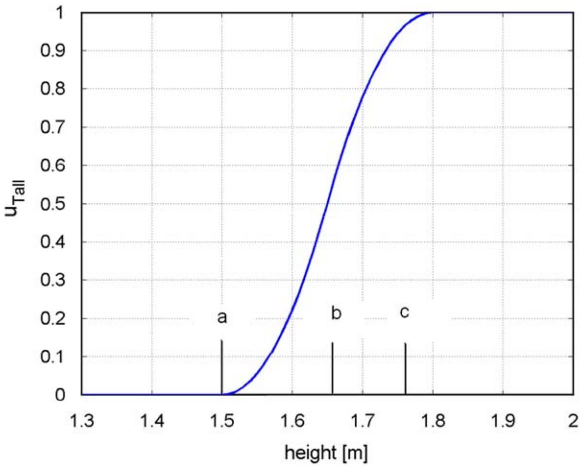

Fig. 2. S-Function.

$$F(x,y) = 1 - T(x,y) \tag{2}$$

where g_{xy} is the intensity value of pixel $P(i,j)$. Variables a, b, and c are the parameters that determine the shape of the S-function as shown in Fig. 2.

Values of parameters a, b, and c can be calculated by using simulated annealing method [22]. However, simulated annealing algorithm is quite time consuming. We will use another histogram based method to calculate a, b, and c [23].

(1) Calculate the histogram of the image.
(2) Find the local maxima of the histogram: $His_{\max}(g_1), His_{\max}(g_2), \ldots, His_{\max}(g_n)$. Calculate the mean of local maxima:

$$\overline{His_{\max}(g)} = \frac{\sum_{i=1}^{n} His_{\max}(g_i)}{n} \tag{3}$$

(3) Find the peaks greater than $\overline{His_{\max}(g)}$, let the first peak be $g_{\min}$ and the last peak be $g_{\max}$.
(4) Define low limit B_1 and high limit B_2:

$$\sum_{i=g_{\min}}^{B_1} His(i) = f_1$$

$$\sum_{i=B_2}^{g_{\max}} His(i) = f_1 \tag{4}$$

where the information loss is allowed in the range $[g_{\min}, B_1]$ and $[B_2, g_{\max}]$, which is f_1 ($f_1 = 0.01$ in the experiments).
(5) Determine a and c:

$$a = (1-f_2)(g_1 - g_{\min}) + g_{\min} \text{if } (a > B_1) \text{ then } a = B_1 \tag{5}$$

$$c = f_2(g_{\max} - g_n) + g_n \text{if } (c > B_2) \text{ then } c = B_2 \tag{6}$$

where $f_2 = 0.01$, and B_1 and B_2 are used to avoid important information loss. The intensity $< B_1$ is considered as background and the intensity $> B_2$ is considered as noise.
(6) Calculate parameter b by using the maximum entropy principal [24]:

$$H(X) = \frac{1}{M \times N} \sum_{i=1}^{M} \sum_{j=1}^{N} S_n(T(x,y)) \tag{7}$$

where $S_n()$ is a Shannon function which is defined as

$$\begin{aligned} S_n(T(x,y)) &= -T(x,y)\log_2 T(x,y) \\ &\quad - (1-T(x,y))\log_2(1-T(x,y))x \\ &= 1,2,\ldots,M, y = 1,2,\ldots,N \end{aligned} \tag{8}$$

Maximum entropy principle: the greater the entropy is, the more information the system includes [9,25,26]. To find the optimal b by trying every $b \in [a+1, c-1]$. The optimal b will result the largest $H(X)$:

$$H_{\max}(X, a, b_{opt}, c) = \max\{H[X; a, b, c] | g_{\min} \le a < b < c \le g_{\max}\} \tag{9}$$

After a, b, and c are determined, the image can be mapped from the intensity domain g_{xy} to the new domain $T(x, y)$. Fig. 3(b) is the result of Fig. 3(a) after mapping.

3.2. Enhancement

Use intensification transformation to enhance the image in the new domain [5]:

$$\begin{aligned} E(T(x,y)) &= 2T^2(x,y) & 0 \le T(x,y) \le 0.5 \\ E(T(x,y)) &= 1 - 2(1-T(x,y))^2 & 0.5 < T(x,y) \le 1 \end{aligned} \tag{10}$$

Fig. 3(c) is the result after enhancement.

3.3. Find the thresholds in *T* and *F*

Two thresholds are needed to separate the new domains T and F. A heuristic approach is used to find the thresholds [5] in T and F.

(1) Select an initial threshold t_0 in T.
(2) Separate T by using t_0, and produces two new groups of pixels: T_1 and T_2, μ_1 and μ_2 are the mean values of these two parts.
(3) Compute the new threshold value: $t_1 = \mu_1 + \mu_2/2$.
(4) Repeat steps 2 through 4 until the difference of $t_n - t_{n-1}$ is smaller than ε (ε=0.0001 in the experiments) in the two successive iterations. Then a threshold t_t is calculated. Fig. 3(d) is the binary image generated by using t_t.

Applying the above steps in F domain, a threshold t_f can be calculated. Fig. 3(e) is the result image by using t_f.

3.4. Define homogeneity in intensity domain and decide {I}

Homogeneity is related to the local information, and plays an important role in image segmentation. We define homogeneity by using the standard deviation and discontinuity of the intensity. Standard deviation describes the contrast within a local region, while discontinuity represents the changes in gray levels. Objects and background are more uniform, and blurry edges are gradually changing from objects to background. The homogeneity value of objects and background is larger than that of the edges.

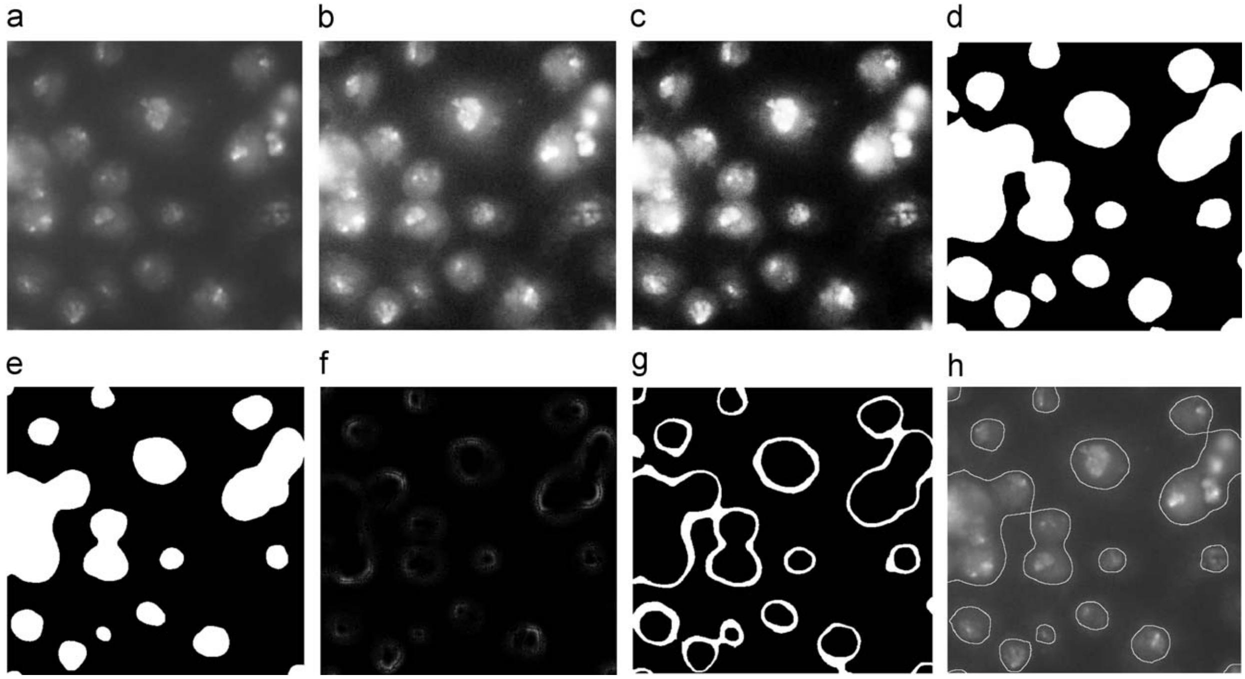

Fig. 3. (a) Cloud image. (b) Result after applying the S-function. (c) Result after enhancement. (d) Image by applying threshold t_t. (e) Image by applying threshold t_f. (f) Homogeneity image in domain I. (g) Binary image based on $\{T, I, F\}$. (h) Final result after applying the proposed watershed method.

A size $d \times d$ window centered at (x, y) is used for computing the standard deviation of pixel $P(i, j)$:

$$sd(x,y) = \sqrt{\frac{\sum_{p=x-(d-1)/2}^{x+(d-1)/2} \sum_{q=y-(d-1)/2}^{y+(d-1)/2} (g_{pq} - \mu_{xy})^2}{d^2}} \tag{11}$$

where μ_{xy} is the mean of the intensity values within the window.

$$\mu_{xy} = \frac{\sum_{p=x-(d-1)/2}^{x+(d-1)/2} \sum_{q=y-(d-1)/2}^{y+(d-1)/2} g_{pq}}{d^2}$$

The discontinuity of pixel $P(i, j)$ is described by the edge value. We use Sobel operator to calculate the discontinuity.

$$eg(x,y) = \sqrt{G_x^2 + G_y^2} \tag{12}$$

where G_x and G_y are the horizontal and vertical derivative approximations.

Normalize the standard deviation and discontinuity, and define the homogeneity as

$$H(x,y) = 1 - \frac{sd(x,y)}{sd_{\max}} \times \frac{eg(x,y)}{eg_{\max}} \tag{13}$$

where $sd_{\max} = \max\{sd(x,y)\}$, and $eg_{\max} = \max\{eg(x,y)\}$.

The indeterminate $I(x, y)$ is represented as

$$I(x,y) = 1 - H(x,y) \tag{14}$$

Fig. 3(f) is the homogeneity image in domain I. The value of $I(x, y)$ has a range of [0,1]. The more uniform the region surrounding a pixel is, the smaller the indeterminate value of the pixel is. The window size should be quite big to include enough local information, but has to be less than the distance between two objects. We choose d=7 in our experiments.

3.5. Convert the image to a binary image based on $\{T, I, F\}$

In this step, we first divide the given image into three parts: objects (O), edges (E), and background (B). $T(x, y)$ represents the degree of being an object pixel, $I(x, y)$ is the degree of being an edge pixel, and $F(x, y)$ is the degree of being a background pixel for pixel $P(x, y)$, respectively. The three parts are defined as follows:

$$O(x,y) = \begin{cases} \text{true} & T(x,y) \geq t_t, I(x,y) < \lambda \\ \text{false} & \text{others} \end{cases}$$

$$E(x,y) = \begin{cases} \text{true} & T(x,y) < t_t \vee F(x,y) < t_f, I(x,y) \geq \lambda \\ \text{false} & \text{others} \end{cases}$$

$$B(x,y) = \begin{cases} \text{true} & F(x,y) \geq t_f, I(x,y) < \lambda \\ \text{false} & \text{others} \end{cases} \tag{15}$$

where t_t and t_f are the thresholds computed in step 3, and $\lambda = 0.01$.

After O, E, and B are determined, the image is mapped into binary image for further processing. We map the objects and background to 0 and map the edges to 1 in the binary image. The mapping function is as following. See Fig. 3(g),

$$Binary(x,y) = \begin{cases} 0 & O(x,y) \vee B(x,y) \vee \overline{E(x,y)} = \text{true} \\ 1 & \text{others} \end{cases} \tag{16}$$

3.6. Apply the watershed to the converted binary image

Watershed algorithm is good for finding the optimal segmentation boundaries. The following is the watershed algorithm for the obtained binary image [5]:

(1) Get regions $R_1, R_2, \ldots, R_n$, which represent the objects and background and have value 0. See Fig. 4.
(2) Dilate these regions by using a 3×3 structure element.
(3) Build a dam at the place where two regions get merged.
(4) Repeat step (3) until all regions merge together. See Fig. 3(h).

4. Experimental results

Watershed segmentation is good for processing nearly uniformed images, and it can get a good segmentation and the edges are connected very well. But this method is sensitive to noise and often has over-segmentation problem [5]. We will compare our method with the pixel-based, edge-based, region-based, and other two watershed methods.

Fig. 5(a) is a cloud image which has blurry boundaries, and Fig. 5(b) is the result by using the pixel-based embedded confidence method [27], which determines the threshold value of a gradient image and consequently performs edge detection. The resulting image is under-segmented and it only detects part of the boundaries. Fig. 5(c) uses Sobel operator which is an edge-based method, it has under-segmentation and the boundaries are not connected well. Fig. 5(d) is the result by using edge detection and image segmentation system (EDISON) which applies mean-shift region-based method [28]. In mean-shift based segmentation, pixel clusters or image segments are identified with unique modes of the multi-modal probability density function by mapping each pixel to a mode using a convergent, iterative process. There are three parameters in EDISON needed to be manually selected: spatial bandwidth, color, and minimum region. We try different combinations of these parameters and get the best result, as shown in Fig. 5(d) (spatial bandwidth=6, color=3, minimum=50). The edges in

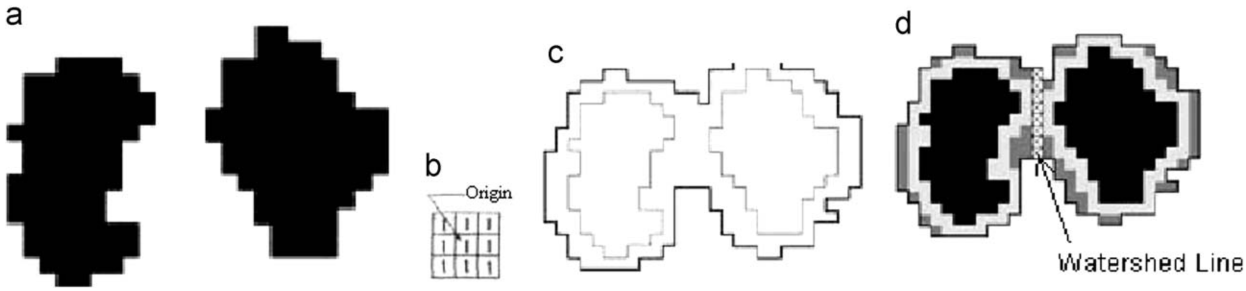

Fig. 4. (a) Two regions which have value 0. (b) 3×3 structure element. (c) Dilation of the two regions. (d) Dam construction.

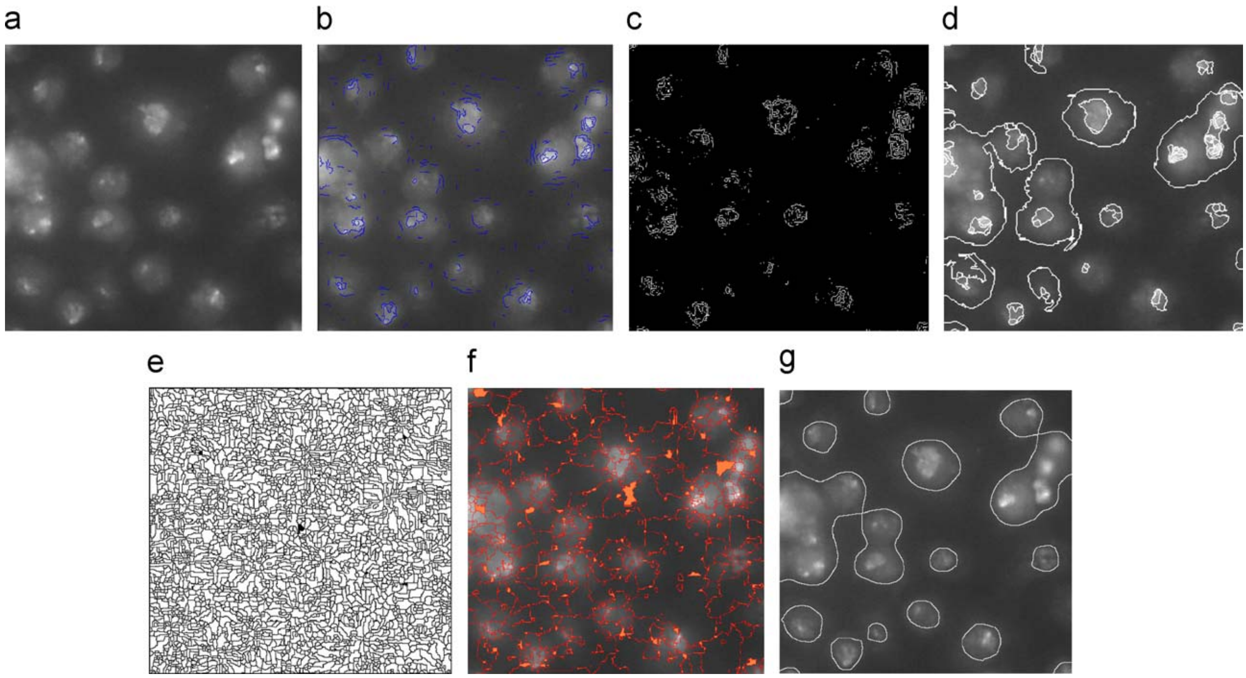

Fig. 5. (a) Original image. (b) Result using the embedded confidence method. (c) Result using the Sobel operator. (d) Result using the mean-shift method. (e) Result using the watershed in Matlab. (f) Result using toboggan-based watershed. (g) Result using the proposed method.

Fig. 5(d) are well connected but not smooth, the result is over-segmented. Fig. 5(e) utilizes the watershed method in Matlab, and the result shows heavy over-segmentation. It is hard to find distinguishable objects. Fig. 5(f) is the result by a modified watershed method (toboggan-based method) [17]. It can efficiently group the local minima by assigning them a unique label. The result is better than Fig. 5(e), but the background and objects are still messed together. Fig. 5(g) applies the proposed method, and it gets clear and well connected boundaries. The result gives an improvement better than those obtained by other methods used in Figs. 5(b–f).

Fig. 6(a) is a blurry cells image. The objects and boundaries are not clear. The edges detected by the embedded confidence method in Fig. 6(b) are discontinued. The Sobel operator in Fig. 6(c) almost

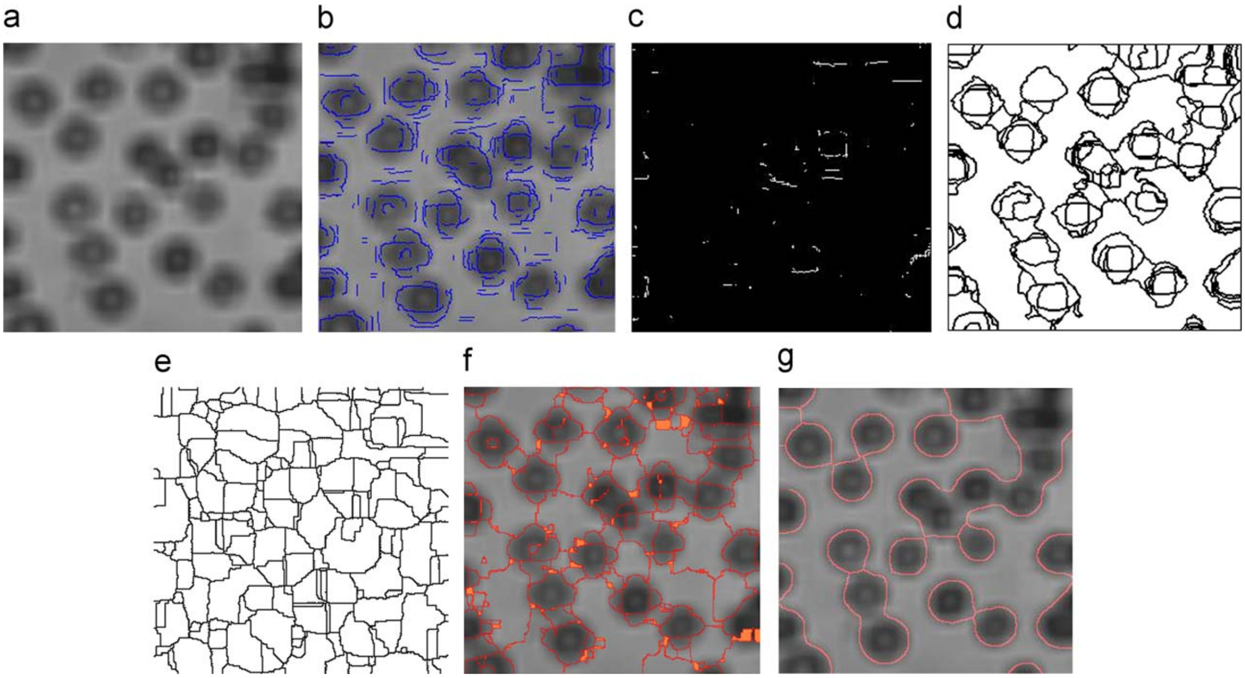

Fig. 6. (a) Blurry cells image. (b) Result using the embedded confidence edge detector. (c) Result using the Sobel operator. (d) Result using the mean-shift method. (e) Result using the watershed in Matlab. (f) Result using the toboggan-based watershed. (g) Result using the proposed method.

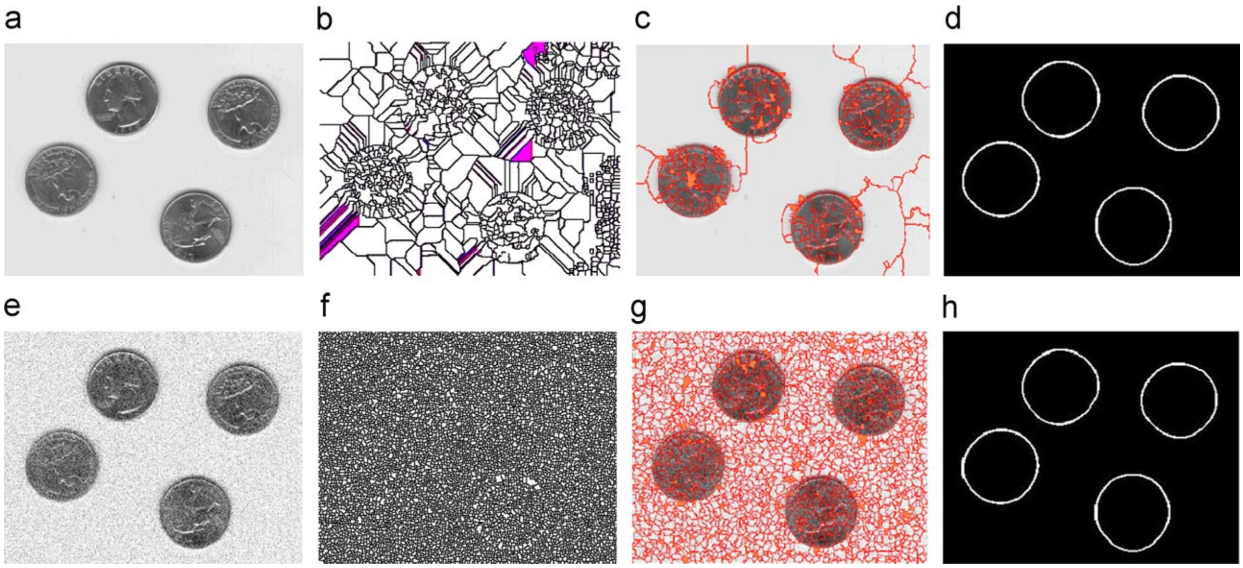

Fig. 7. (a) Original image. (b) Result using the watershed in Matlab on the original image. (c) Result using the toboggan-based watershed on the original image. (d) Result using the proposed method on the original image. (e) Image added with Gaussian noise. (f) Result using the watershed in Matlab on the noisy image. (g) Result using the toboggan-based watershed on the noisy image. (h) Result using the proposed method on the noisy image.

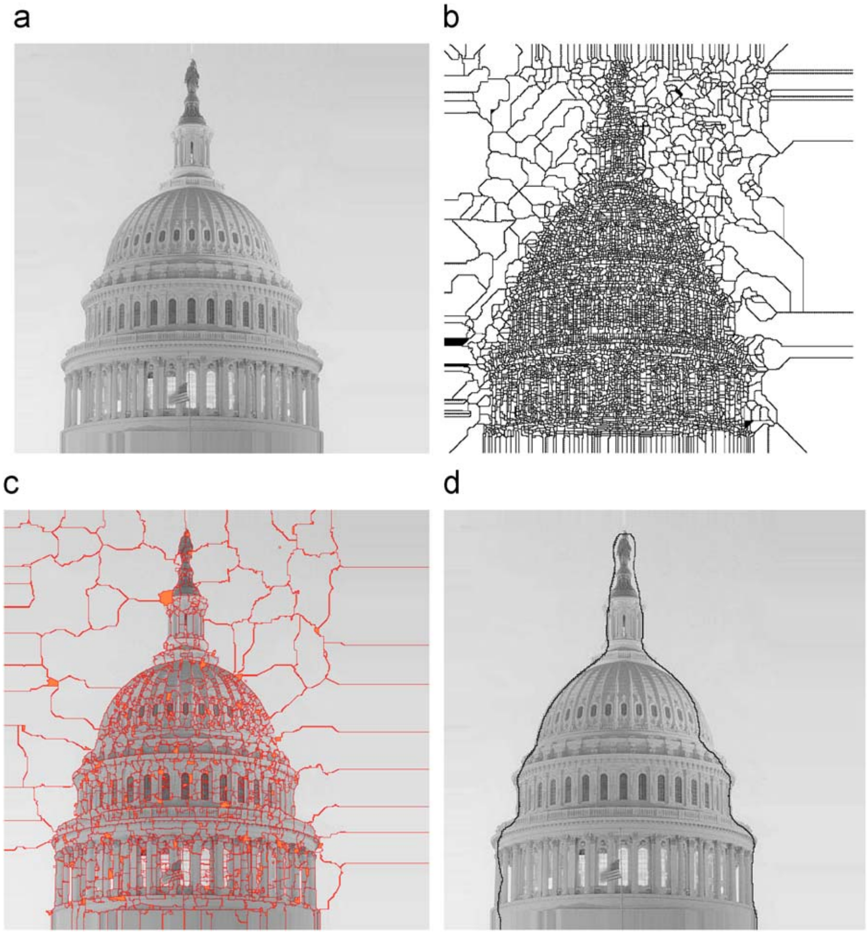

Fig. 8. (a) Original capitol image. (b) Result using the watershed in Matlab. (c) Result using the toboggan-based method. (d) Result using the proposed method.

loses all boundaries. The mean-shift method in Fig. 6(d) (spatial bandwidth=7, color=3, minimum=10) produces few connected edges, and the edges are not well detected. Two watershed methods in Figs. 6(e, f) produce over-segmentation. The result in Fig. 6(g) using the proposed method has well connected and clear boundaries to segment the cells from the background better.

One drawback of the watershed methods is noise sensitive. However, the proposed method is very noise-tolerant. Fig. 7(a) is a noise-free coin image, and Figs. 7 (b–d) are the results by employing the watershed method in Matlab, toboggan-based watershed method, and the proposed neutrosophic watershed method, respectively. Fig. 7(e) is the image by adding Gaussian noise (mean is 0, and standard variance is 2.55) to Fig. 7(a). Figs. 7(f–h) are the results by applying the above three watershed methods to Fig. 7(e). We can see that the Gaussian noise has a big impact on the results using the existing watershed methods, and causes heavy over-segmentation. But the proposed neutrosophic watershed method is quite noise-tolerant.

Another problem of the existing watershed algorithms is that they do not work well for non-uniform images. In Fig. 8(a), the capitol has a wide range of intensities. The top of the capitol is dark, the middle part of the capitol is gray, and the bottom part of capitol is white. Fig. 8(b) is the result by applying the watershed method in Matlab and Fig. 8(c) is the result by applying toboggan-based watershed method. Both of them do not work well. Fig. 8(d) is the result by applying the proposed method and the capitol can be segmented well.

5. Conclusions

In this paper, we propose a novel watershed image segmentation approach based on neutrosophic logic. In the first phase, we map a given image to three subsets T, F, and I, which are defined in different domains. The thresholding and neutrosophic logic are employed to obtain a binary image. Finally, the proposed watershed method is applied to get the segmentation result. We compare our method with the pixel-based, edge-based, region-based segmentation methods, and two existing watershed methods. The experiments show that the proposed method has better performance on noisy and non-uniform images than that obtained by using other watershed methods, since the proposed approach can handle the uncertainty and indeterminacy better. It may find more applications in diverse fields of control theory, image processing, computer vision, and artificial intelligence.

References

[1] F. Smarandache, A Unifying Field in Logics Neutrosophic Logic. Neutrosophy, Neutrosophic Set, Neutrosophic Probability, American Research Press, New York, 2003.

[2] H.D. Cheng, Y. Guo, A new neutrosophic approach to image thresholding, New Mathematics And Natural Computation 4 (2008) 291–308.

[3] Y.H. Guo, H.D. Cheng, J. Tian, Y.T. Zhang, A novel approach to speckle reduction in ultrasound imaging, Ultrasound in Medicine and Biology 35 (2009) 628–640.

[4] L.A. Zadeh, Fuzzy sets, Information and Control 8 (3) (1965) 353–383.

[5] R.C. Gonzalez, R.E. Woods, Digital Image Processing, second ed., Prentice-Hall, New York, 2002.

[6] L.G. Shapiro, G. Stockman, Computer Vision, Prentice-Hall, New Jersey, 2001.

[7] H. Zhang, J.E. Frittsb, S.A. Goldmana, Image segmentation evaluation: a survey of unsupervised methods, Computer Vision and Image Understanding 110 (2008) 260–280.

[8] Y. Jiang, Z.-H. Zhou, SOM ensemble-based image segmentation, Neural Processing Letter 20 (2004) 171–178.

[9] N.R. Pal, S.K. Pal, A review in image segmentation techniques, Pattern Recognition 26 (1993) 1277–1294.

[10] R.M. Haralick, L.G. Shapiro, Survey: image segmentation techniques, Computer Vision, Graphics and Image Processing 29 (1985) 100–132.

[11] A. Bleau, L.J. Leon, Watershed-based segmentation and region merging, Computer Vision and Image Understanding 77 (2000) 317–370.

[12] P. Li, X. Xiao, Multispectral image segmentation by a multichannel watershed-based approach, International Journal of Remote Sensing 28 (2007) 4429–4452.

[13] L. Najman, M. Couprie, G. Bertrand, Watersheds, mosaics, and the emergence paradigm, Discrete Applied Mathematics 147 (2005) 301–324.

[14] L. Najman, M. Schmitt, Geodesic saliency of watershed contours and hierarchical segmentation, IEEE Transactions on Pattern Analysis and Machine Intelligence 18 (1996) 1163–1173.

[15] L. Najman, M. Schmitt, Watershed of a continuous function, Signal Processing (Special issue on Mathematical Morphology) 38 (1994) 99–112.

[16] D. Wang, A multiscale gradient algorithm for image segmentation using watersheds, Pattern Recognition 30 (1997) 2043–2052.

[17] Y.C. Lin, Y.P. Tsai, Y.P. hung, Z.C. Shih, Comparison between immersion-based and toboggan-based watershed image segmentation, IEEE Transactions on Image Processing 15 (3) (2006) 632–640.

[18] K. Atanassov, Intuitionistic fuzzy sets, Fuzzy Sets and Systems 20 (1986) 87–96.

[19] G. Priest, Paraconsistent logic, in: Handbook of Philosophical Logic, vol. 6, Kluwer Academic Publishers, Dordrecht, 2002.

[20] W. Bruno, Dialetheism, logical consequence and hierarchy, Analysis 64 (2004) 318–326.

[21] P.A. Loeb, M. Wolff, Nonstandard Analysis for the Working Mathematician, Kluwer, Dordrecht, Netherlands, 2000.

[22] H.D. Cheng, J.R. Chen, Automatically determine the membership function based on the maximum entropy principle, Information Sciences 96 (1997) 163–182.

[23] H.D. Cheng, J.L. Wang, X.J. Shi, Microcalcification detection using fuzzy logic and scale space approach, Pattern Recognition 37 (2004) 363–375.

[24] H.D. Cheng, J.G. Li, Fuzzy homogeneity and scale space approach to color image segmentation, Pattern Recognition 35 (2002) 373–393.

[25] H.D. Cheng, H. Xu, A novel fuzzy logic approach to contrast enhancement, Pattern Recognition 33 (2000) 809–919.

[26] S.K. Pal, D.K.D. Majumder, Fuzzy Mathematical Approach to Pattern Recognition, Wiley, New York, 1986.

[27] P. Meer, B. Georgescu, Edge detection with embedded confidence, IEEE Transactions on Pattern Analysis and Machine Intelligence 23 (2001) 1351–1356.

[28] D. Comaniciu, P. Meer, Mean shift: a robust approach toward feature space analysis, IEEE Transactions on Pattern Analysis and Machine Intelligence 24 (2002) 603–609.